JOURNAL OF PROPULSION AND POWER
Vol. 17, No. 3, May–June 2001

# Parametric Study of the Swirler/Venturi Spray Injectors

Kyoung-Su Im,* Hoisan Kim,† and Ming-Chia Lai‡
*Wayne State University, Detroit, Michigan 48202*
and
Robert Tacina§
*NASA John H. Glenn Research Center at Lewis Field, Cleveland, Ohio 44135*

**An experimental parametric study is carried out to characterize the spray from swirler/venturi injectors (SVIs) inside a steady-flow pressure chamber. In this study, venturi tubes with diffuser angles of 20, 40, 60, and 80 deg and different throat lengths are combined with different swirlers with vane angles of 30, 45, and 60 deg to investigate their combined effect on spray structure. The ambient pressure conditions inside the chamber were varied from 0.1 to 0.4 MPa to simulate the relevant gas turbine density and momentum condition. For simplicity, water is used to present liquid fuel. Focusing on the spray atomization and dispersion aspects, laser diagnostic techniques are used to characterize the isothermal spray structure, including phase Doppler particle analyzer and copper-vapor laser-sheet visualization. Pressure drop across the SVI is also measured. It was found that the pressure drop and droplet size are dominated by the throat velocity, but are modified significantly by the divergent angle, throat length, and swirler. It is also shown that matching the correct swirler with the venturi geometry is important to obtain optimal liquid atomization and droplet distribution.**

## Introduction

A SWIRLER/VENTURI injector (SVI) is a generic combination of a swirler and a tube injector, in which liquid-fuel is injected through a capillary tube at the throat section of a venturi tube, to maximize atomization performance due to aerodynamic breakup mechanism. Similar to automotive carburetors, this requires only a very modest fuel pump pressure. The diffuser (divergence) section of the venturi tubes is designed to recover the pressure head as well as to enhance fuel–air mixing, but without creating recirculation regions where autoignition could take place before the desired flame-holding locations. To obtain better atomized spray and more uniform fuel–air mixture, a venturi combined with swirler and a multiple venturi fuel injector have been proposed and are considered to have an advantage over the venturi-tube-only fuel injection system. Multiple SVI elements can be combined into a integrated unit and used as a fuel premixer. The resultant improvement in atomization, evaporation, and mixing of fuel in combustion air has potential applications in ultra-low-$NO_x$ gas turbine combustors.

There has been great interest in reducing the $NO_x$ emission because atmospheric pollution has become a worldwide concern. Numerous researchers have confirmed that the attainment of drastically reduced $NO_x$ levels, by using advanced combustor design concepts, is the most formidable emission abatement technology challenge associated with gas turbine engines. The basic factors influencing the formation of $NO_x$ are combustion temperature, residence time of combustion species in the high-temperature zone, and fuel–air ratio in the combustion zone.

The most common approaches proposed to reduce $NO_x$ emissions are listed as follows.

1) Utilization of water-in-oil emulsified by fuel or by water or steam secondary injection can significantly decrease the heterogeneity and temperature of the fuel–air mixture. It has been shown to be effective, but this method has some undesirable side effects, such as lower thermodynamic efficiency of the combustion process.

2) Selective catalytic reduction, such as injecting ammonia into the gas turbine exhaust stream to reduce $NO_x$ in the presence of a catalyst converter to $N_2$ and $H_2O$, can remove most of the $NO_x$ (Ref. 1), but requires that the exhaust gas temperature remain in a narrow range. Like water injection, it is also limited to ground-based turbines.

3) Use of a variable-geometry combustor such as the rich-burn quick-quench lean-burn process is shown to be a stable process, but its quick mixing stage is very critical,[2,3] and the resultant $NO_x$ reduction is not the lowest possible.

4) Lean premixed-prevaporized (LPP) combustion yields the lowest $NO_x$. Cooper[4] has claimed that LPP is a potential method for obtaining superior performance, high durability, and low pollutant emissions. Correa[5] has concluded that the lean premixed combustion is probably the only combustion technology that will reduce $NO_x$ emission. Lefebvre[6] has predicted that an LPP combustor would be the most promising system and could drastically reduce $NO_x$ emission due to the low reaction temperature and elimination of hot spots in the combustion zone. Also, extensive research has been reported recently on LPP combustion to reduce $NO_x$ emission.[7–12] The success of the dry, low-$NO_x$ LPP combustion process depends critically on the fuel–air vaporizing-mixing stage and the flame-holding stage.

Earlier flame tube experiments[4,13–15] at NASA examined the performance of different types of multiple source injectors. The degree of liquid fuel vaporization was determined using a spillover sampling technique. The multiple conical (venturi) injector was found to yield better fuel evaporation under test conditions (0.3 MPa and up to 700 kPa). A simple mechanism that accounts for the combustion of liquid droplets in partially vaporized mixtures was found to predict $NO_x$ data with fair accuracy.

Johnson[16] illustrated the effect of venturi configuration by comparing the droplet size data of a conventional simplex conical spray injector mounted with a mixing venturi to data without the venturi. The drop measurements using laser scattering techniques suggested that significant improvement in atomization with the venturi configuration was the main reason for reductions in $NO_x$ emission in the combustion experiments.[13,17] Adding a divergent tube to a traditional airblast plain jet[18] with improved atomization provided more time for vaporizing and mixing with air. The experimental results by Ercegovic[17] on a swirler-combined mixing venturi using jet-A fuel showed that $NO_x$ was remarkably reduced as a result of the

Received 28 March 2000; revision received 28 September 2000; accepted for publication 18 October 2000. 

*Research Associate, Department of Mechanical Engineering; ksim@fluid.eng.wayne.edu. Member AIAA.

†Ph.D. Student, Department of Mechanical Engineering; hoisan@fluid.eng.wayne.edu.

‡Professor, Department of Mechanical Engineering; lai@eng.wayne.edu. Member AIAA.

§Senior Scientist, Combustion Branch, Turbomachinery and Propulsion Systems Division; Robert.R.Tacina@grc.nasa.gov. Member AIAA.

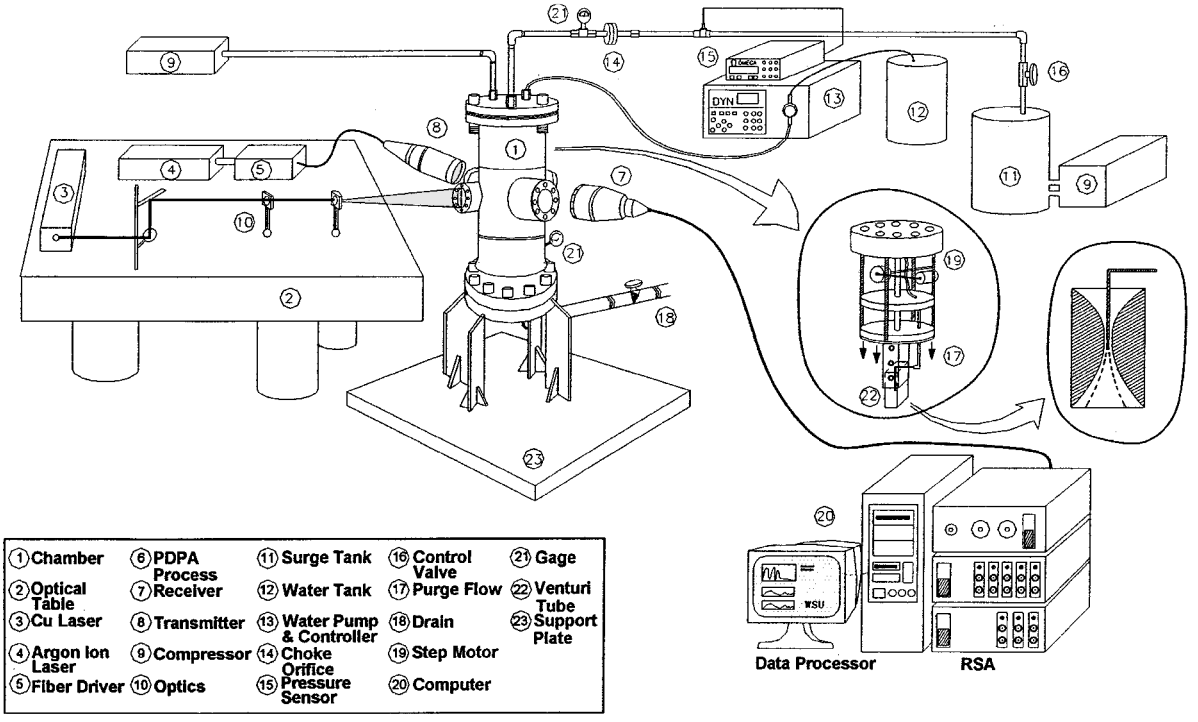


**Fig. 1 Schematic of the venturi nozzle spray system.**

introduction of the swirler, indicating finer atomization, more complete vaporization, and better mixing. Also, a multiple venturi tube configuration showed the possibility of obtaining a more homogeneous fuel–air mixture, modest fuel pump pressure requirements, and uniform temperature distribution, and, therefore, low soot and HC formation and lower $NO_x$ emission.[19]

Zheng et al.[20] focused their research on the structure of airblast sprays under ambient pressure conditions, such as 0.1, 0.6, and 1.2 MPa, where they used a prefilming airblast atomizer. They reported that increasing the ambient pressure at constant fuel–air ratio caused the initial spray cone angle to widen, but downstream, the spray volume remained largely unaffected by the ambient pressure.

Parsons and Jasuja[21] examined the spatial distribution characteristics of fuel sprays emanating from simplex pressure swirl atomizers of the type commonly used in the gas turbine engine, using a nonintrusive photographic technique. They developed the correlated expressions between the spray half width $y$, gas pressure $P_a$, and fuel pressure drop $\Delta P_f$.

Optical techniques such as the phase Doppler particle analyzer (PDPA)[22] and planar laser-induced fluorescence (PLIF) visualization systems[13] have been developed for spray diagnostics. Also, breakup models[23–25] have been implemented in multidimensional spray modeling.

In most previous experiments using a venturi injector, the atomization and vaporization history was not characterized in detail. Only very limited experimental and analytical data on the basic fuel–air processes in this type of injector are available for practical design purposes.

Recently, Sun et al.[26,27] investigated the atomization and vaporization characteristic of airblast fuel injection inside a venturi tube using PDPA and PLIF techniques. Different shapes of venturi (freejet, straight, and venturi nozzles with swirler) tubes were used to illustrate the uniform fuel–air mixture and atomization. Compared with the freejet and straight tube nozzle spray, the venturi nozzle spray produces the most uniform fuel–air mixture. Incorporating swirl into the venturi tube design could result in further improvement of the spray.

In this study, which serves as an extension of previous work,[26] a parametric study was carried out of swirler/venturi nozzle combinations (30–60 deg blade angle) for capillary liquid injection in a coflowing airstream inside a single venturi tube. In addition, various venturi and swirler combinations were tested to determine the optimal configuration for various flow and pressure conditions.

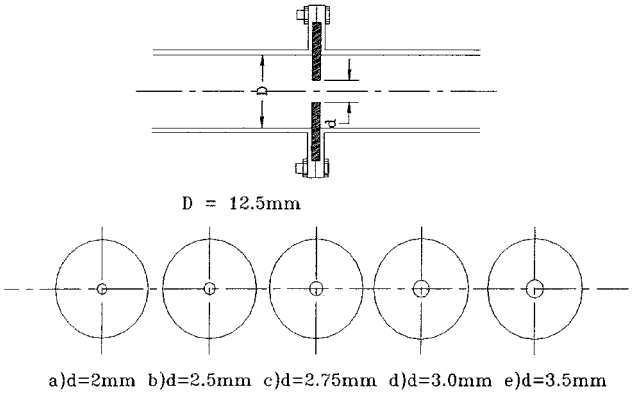


**Fig. 2 Choked orifice and different orifice coins.**

## Experimental Setup

The experimental setup is shown in Fig. 1. Compressed air from a 1140 L reservoir at 3.45 MPa is used as the gas supply. The flow rate of the gas is controlled by a pressure regulator and is monitored by an Omega FC-20 flow computer, complete with a platinum resistance thermometer (FR-12-2-100), a silicon piezoresistive pressure transmitter (PX-880), and a vortex flowmeter (FV-505). To maintain a steady flow condition at different pressures inside the chamber, a critical flow orifice (CFO) metered the atomization airflow upstream of the pressurized chamber. The different CFO hole sizes are shown in Fig. 2.

For an incremental flow range, different orifices were used to maintain the choked pressure criterion, that is, the upstream pressure is more than twice that of the downstream pressure, which was measured downstream of the choked orifice. Water at room temperature is continuously injected into the high-speed airstream at the venturi throat through a capillary tube having a 0.355-mm inner diameter. The flow rate of the water is controlled by a Dynamax SD-200 precision liquid pump system and is displayed on a monitor. The spray injection assembly is mounted on a two-dimensional, stepper-motor-controlled traversing stage, which is inside the pressure chamber. To establish a uniform airflow inside the venturi tube,

**Table 1 Specification of the venturi nozzle geometry**

| Diffuser angle $\alpha$, deg | Convergence length $L_1$, mm | Divergence length $L_2$, mm |
|---|---|---|
| | *$L_{th} = 12.7$, throat* | |
| 10 | 25.4 | 54.02 |
| 20 | 25.4 | 26.162 |
| 30 | 16.51 | 16.51 |
| 40 | 11.43 | 11.43 |
| | *$L_{th} = 0.0$, no throat* | |
| 10 | 25.4 | 54.02 |
| 20 | 25.4 | 26.162 |
| 30 | 16.51 | 16.51 |
| 40 | 11.43 | 11.43 |

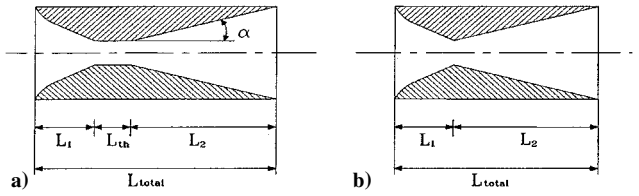


**Fig. 3 Geometry of the venturi nozzle: a) without throat length and b) with throat length.**

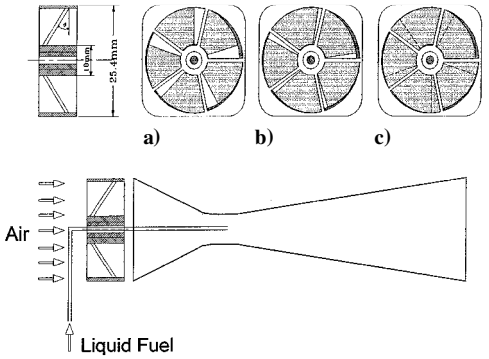


**Fig. 4 Air swirler of inclined blade angle relative to airflow direction venturi/swirler: a) 30, b) 45, and c) 60 deg.**

a honeycomb flow straightener ($25.4 \times 25.4 \times 50$ mm) was mounted upstream of the swirler entrance.

When the airflow rate and the ambient chamber pressure increase, the spray droplets impinge inside of the chamber wall and obscure the optical windows very quickly, making spray visualization and PDPA measurement difficult. Therefore, an annular purge flow system is introduced to reduce the recirculation of the spray droplets and their wall impingement onto the optical windows. However, this purge flow does not affect the atomization airflow rate because it is controlled by a CFO, which is independent of downstream pressure.

A total of eight venturis, with and without throat length, having different divergent angles was tested. The basic geometry of the venturi nozzle is shown in Fig. 3, and the dimensions of the nozzles are summarized in Table 1. For each venturi nozzle, four swirler conditions are tested: three swirlers with vane angles $\theta$ of 30, 45, and 60 deg (Fig. 4) and a baseline case without any swirler. The effected flow area, as defined by the annular area between the tube and the hub, however, is not the same: 540 mm$^2$ for $\theta = 30$ and 45 deg and 250 mm$^2$ for $\theta = 60$ deg.

The pressure of the spray chamber is controlled by the throttle valve located at the bottom part of the chamber and is checked by a pressure gauge from the spray chamber. For each throat velocity, the ambient chamber pressure was changed from 0.1 to 0.4 MPa. The transparent quartz windows on the chamber wall were used for the visualization photograph and to measure droplet size.

For spray visualization, a copper vapor laser (Oxford 15A) is used as a light source. The pulsed laser light sheet, about 1 mm in thickness, was introduced into the spray chamber through the transparent quartz window and vertically illuminated the spray flowfield. A 35-mm still camera (Nikon FM2) was used to record the image. The camera is connected with an N-shot controller, which determines the number of laser light pulses. Each photograph was taken for 20–30 pulses at 3 kHz in this study.

A two-channel PDPA (Aerometrics) was used to measure droplet size, velocity, and volume flux of the water spray. As shown in Fig. 1, two intersecting laser beams emanate from the transmitter and intersect the focal point of the transmitting lens. A 2-W argon-ion laser, at 488- and 514.5-nm wavelengths, was used as the light source. The focusing lenses of both the transmitter and the receiver have a long focal length of 250 mm. All of the PDPA measurements were carried out at the same sampling time of 40 s. Statistics at each point are averaged over 10,000 data points. The validation rate was higher than 90% for every measuring point.

The throat velocity was varied from 50 to 200 m/s, with the ambient chamber pressure varying from 0.1 to 0.4 MPa. This corresponds to an air mass flow rate of 1.76–24.4 g/s. The water injection rate was also varied proportionally to keep the air–liquid mass equivalence ratio at 1.0 (stoichiometric condition) for different airflows.

## Results and Discussion

### Pressure Loss

An ideal fuel prevaporizing system should be able to provide uniform fuel concentration, velocity distribution, complete vaporization, and low pressure loss. The length of the tube should be long enough to allow droplets to have sufficient time to vaporize. However, long residence time may also increase the probability of autoignition and flashback inside the tube. Therefore, the residence time should be less than the autoignition delay time. To reduce the probability of autoignition or flashback, the air speed at the throat area of venturi tube should be sufficiently high under any circumstances. In addition to complete vaporization, the advantage of using the venturi tube is to provide pressure recovery. The main factors in assessing combustion chamber performance are pressure loss, combustion efficiency, and stability limits. Any pressure drop between the inlet and the outlet of the combustion chamber leads to reduction of output power and thermal efficiency.

Figure 5 shows the pressure drops across each venturi tube as a function of the flow velocity at the venturi throat, which is maintained at a prescribed flow condition. As expected, the pressure drop across the SVI increases with velocity, but not quite quadratically. Surprisingly, the swirler has little effect on the pressure drop for larger diffuser angle, that is, the swirler does not contribute to the pressure drop significantly for the shorter diffuser. Therefore, the pressure drop in the shorter SVI is dominated by the maximum area contraction, which is from the unrestricted flow area before the swirler to the bottleneck at the venturi throat. Only the pressure drop for the 20-deg venturi shows significant sensitivity with a different swirler. As expected, the venturi tube with a long diffuser reveals good pressure recovery. In addition, the baseline (no swirler) pressure drop is reduced when combined with a $\theta = 30$ deg swirler upstream. This shows that these swirlers effectively prevent the diffuser flow from the separation, which stalled the diffuser in the baseline case. However, the $\theta = 45$ and 60 deg swirlers increase the diffuser pressure drop by their overly large swirl momentum and smaller effective area. Therefore, if minimum pressure drop is the absolute criterion, then a 20-deg venturi combined with a $\theta = 30$ deg swirler is the best geometry.

Figure 6 shows another aspect of the pressure drop by replotting the data in Fig. 5 with respect to divergence angle. Comparing Figs. 5a and 6a with Figs. 5b and 6b, it is clear that a finite throat length can contribute to better pressure recovery because the pressure drop for those venturi tubes with a finite throat length is smaller than the pressure drop without throat length for every divergence angle. This may be because a finite throat length provides a smoother flow transition at the throat. In addition, although pressure in general increases with diffuser angle $\theta$, cases with a finite throat length seem to have a maximum around $\theta = 60$ deg. Note that the highest rate of pressure-loss increase arises at a divergent angle between 20 (54.02-mm divergence length) and 40 deg (26.162-mm divergence length).

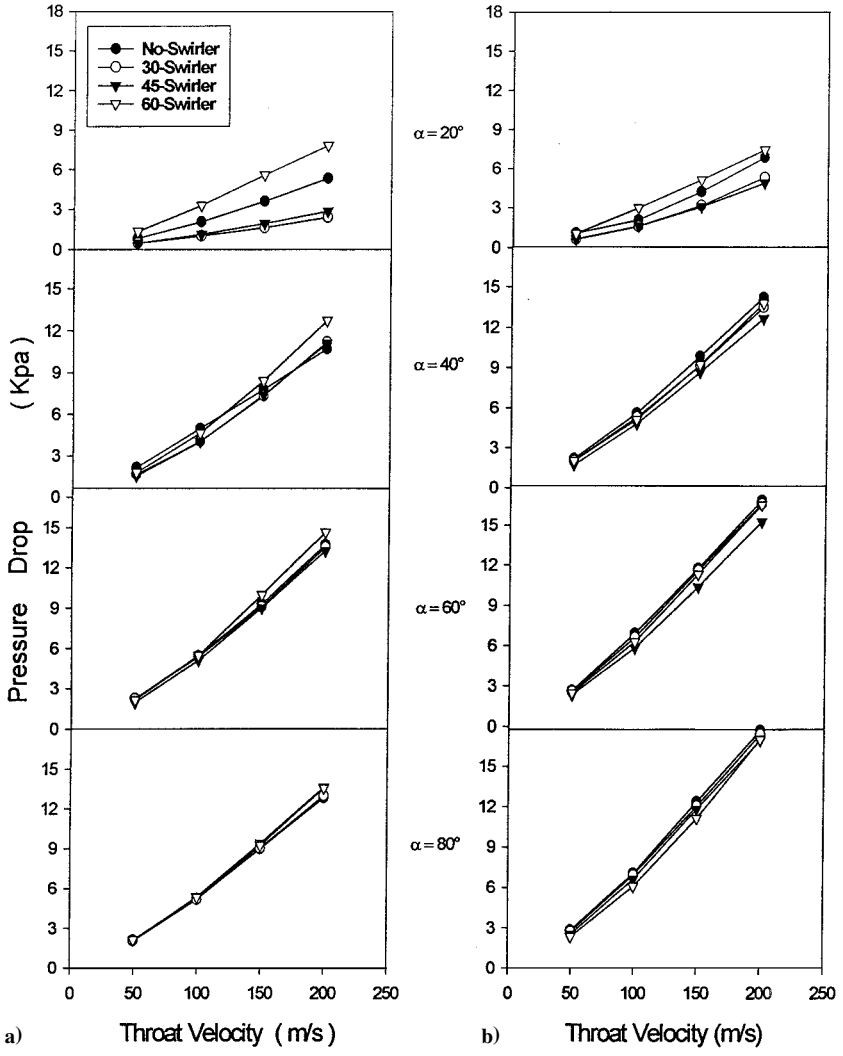


**Fig. 5 Pressure drop across the venturi nozzle for $\alpha$ = 20-, 40-, 60-, and 80-deg divergence angle from top: a) with throat length and b) without throat length.**

**Spray Structure**

The spray structure is characterized both by spray visualization using laser light-sheet illumination and by PDPA measurements.

The parameters governing the atomization performance of air-blast atomizers include the physical properties of air and the liquid used, for example, density, viscosity, and surface tension; the dynamic properties of flowfield, for example, relative velocity, ambient pressure and density, and air–liquid flow rate; and the geometry of the spray nozzle, for example, the divergent angle $2\alpha$ and the swirler angle $\theta$. In this study, a wide range of conditions was covered, except for a constant air–liquid ratio and constant liquid properties. Limited by available space, only representative data sets are discussed in the paper.

The general characteristics for the SVI spray are shown in Figs. 7–9 for a $2\alpha = 40$ deg venturi geometry with an averaged air velocity of 100 m/s at the throat. Figure 7 shows the spray visualization images, Fig. 8 the two-dimensionsal velocity profiles of the overall spray, and Fig. 9 the corresponding to mean droplet size profiles for each condition. Comparing Fig. 7a with Fig. 7b, a long-throat venturi has a wider spray than a sharp-throat, that is, without throat length, venturi. Figures 8a and 8b also show that a long-throat venturi has a slightly narrow velocity profile. The large dynamic range of the SMD was observed in Fig. 9a for the sharp-throat venturi. Figure 9 also shows that it has larger droplet at the center of the spray compared to the long-throat nozzle and slightly smaller droplet size at the spray peripheral. Therefore, it is obvious from the experimental results that a finite throat length not only has lower pressure drop benefits, but it can also contribute to the atomization and fuel–air mixing by a longer residence time at the high-speed atomization regime.

## Characteristics of Venturi Tube Spray

The swirler effects on the venturi nozzle spray are clearly shown by comparing Figs. 7b, 8b, and 9b with Figs. 7c, 8c, and 9c. The spray pattern is widened significantly, and the velocity profiles become more uniformly distributed. The drop size is reduced at the center of the spray; for the $2\alpha = 40$ deg venturi geometry shown, its distribution also becomes more uniform along the radial direction. This atomization improvement is attributed to the confined swirling airflow inside the venturi increasing shearing air velocity at the venturi throat.[28]

It is well known that changing ambient pressure influences spray angle or spray width, but there have been different conclusions as to whether the spray angle is wider or narrower with increasing ambient pressure. When Figs. 7d, 8d, and 9d are compared with Figs. 7b, 8b, and 9b, doubling the ambient pressure from 0.1 to 0.2 MPa does not appear to change the spray boundary much, but may increase the spray density especially near the nozzle exit based on spray intensity. More interesting, the velocity profile near the exit shows a wakelike profile, with a velocity deficit at the center of the spray. Farther downstream, however, it shows a more uniform profile. The effects of venturi geometry, swirler, ambient pressure, and air velocity are further discussed in detail.

Figure 10 shows the effect of the venturi geometry at 100-m/s throat air velocity, 0.1-MPa ambient pressure, with divergent angles

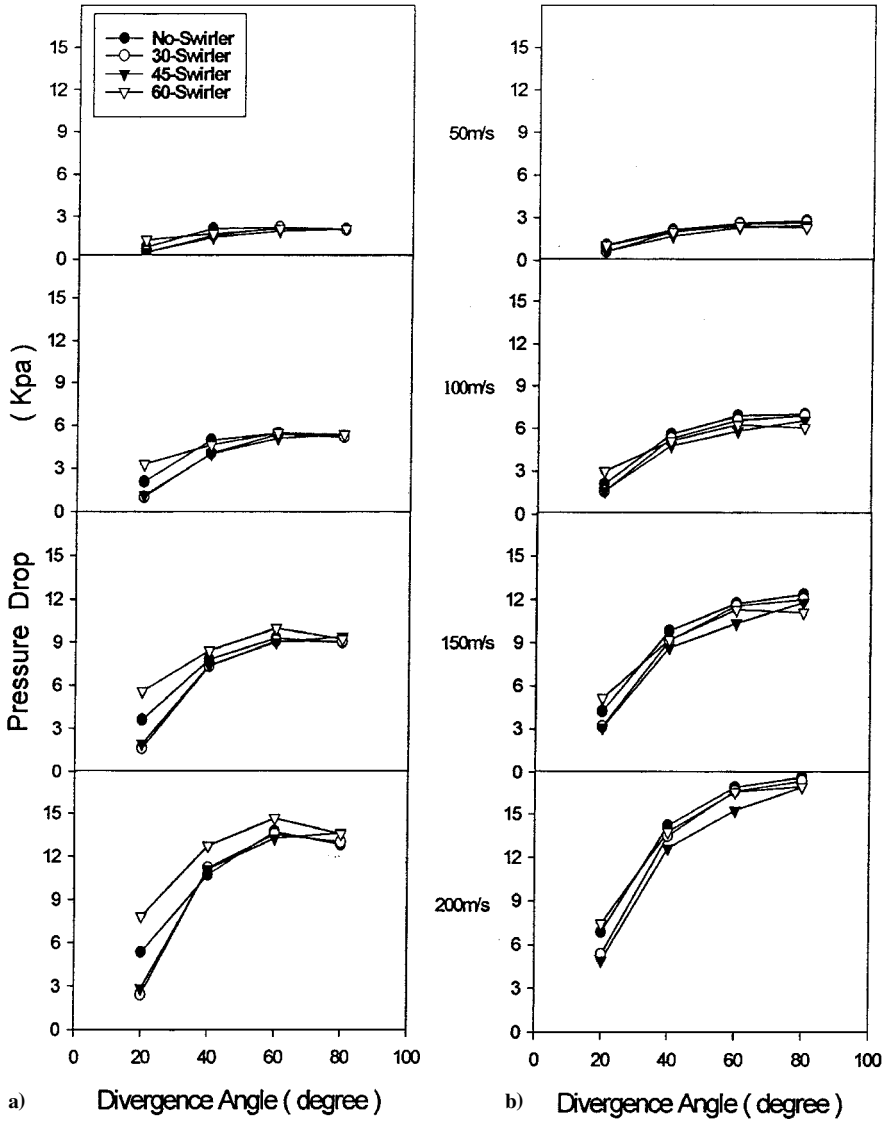


**Fig. 6 Pressure drop across the venturi nozzle for 50-, 100-, 150-, and 200-m/s throat velocity from top: a) with throat length and b) without throat length.**

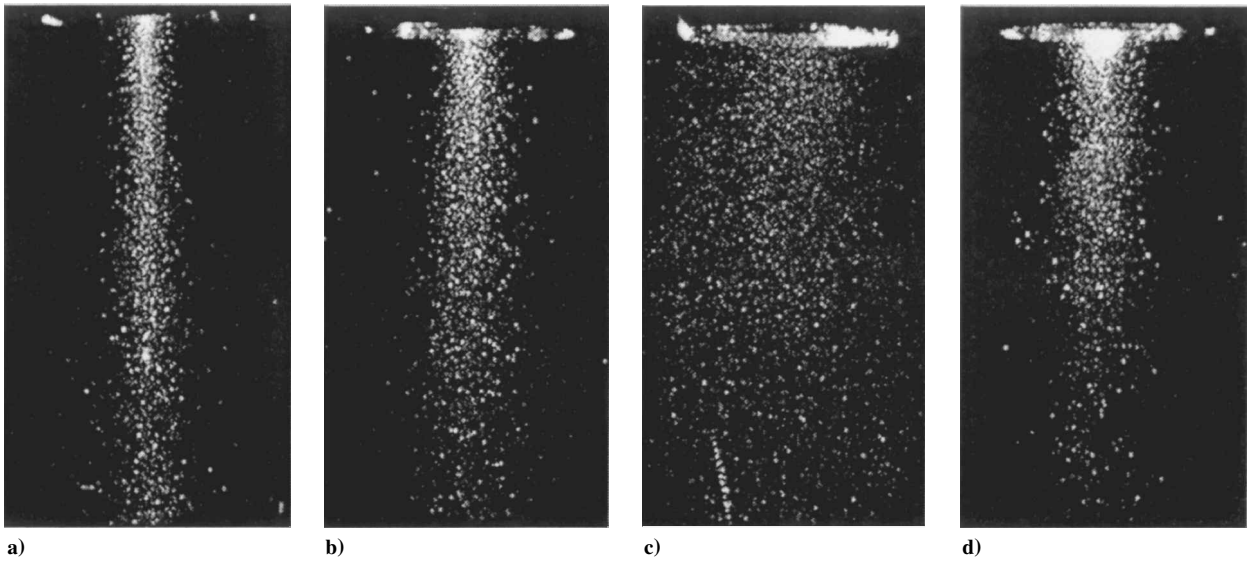


**Fig. 7 Photograph of the 40-deg divergent angle venturi at air velocity 100 m/s: a) without throat length, b) with throat length, c) combined 30-deg swirler, and d) 0.2-MPa chamber pressure on the throat length venturi.**

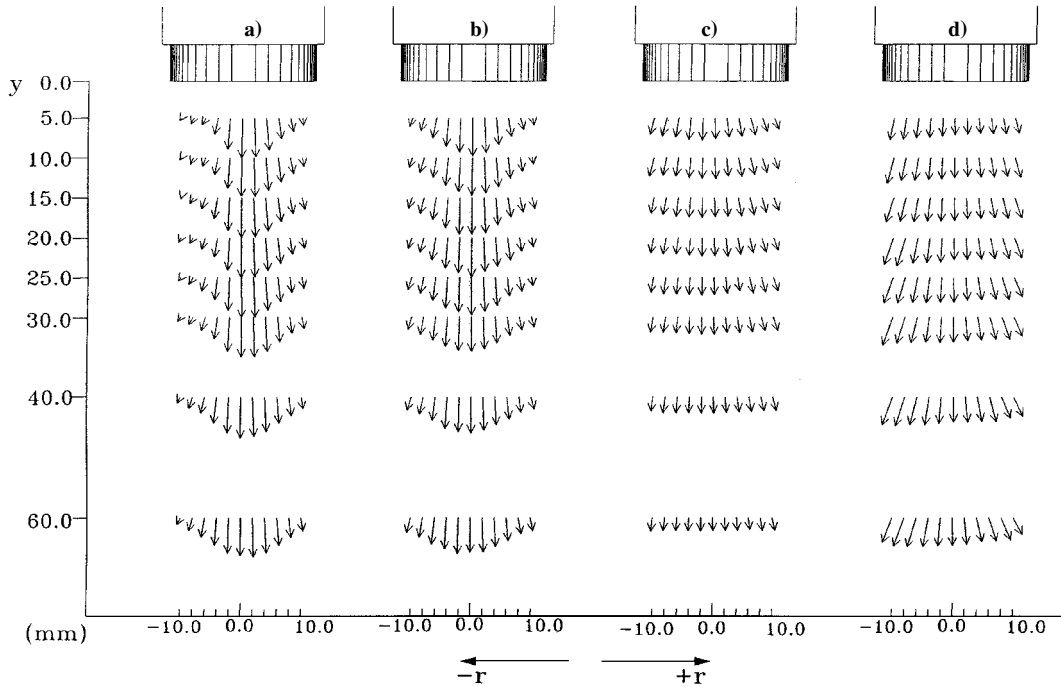


**Fig. 8 Velocity distributions of the 40-deg divergent angle venturi at air velocity 100 m/s: a) without throat length, b) with throat length, c) combined 30-deg swirler, and d) 0.2-MPa chamber pressure on the throat length venturi.**

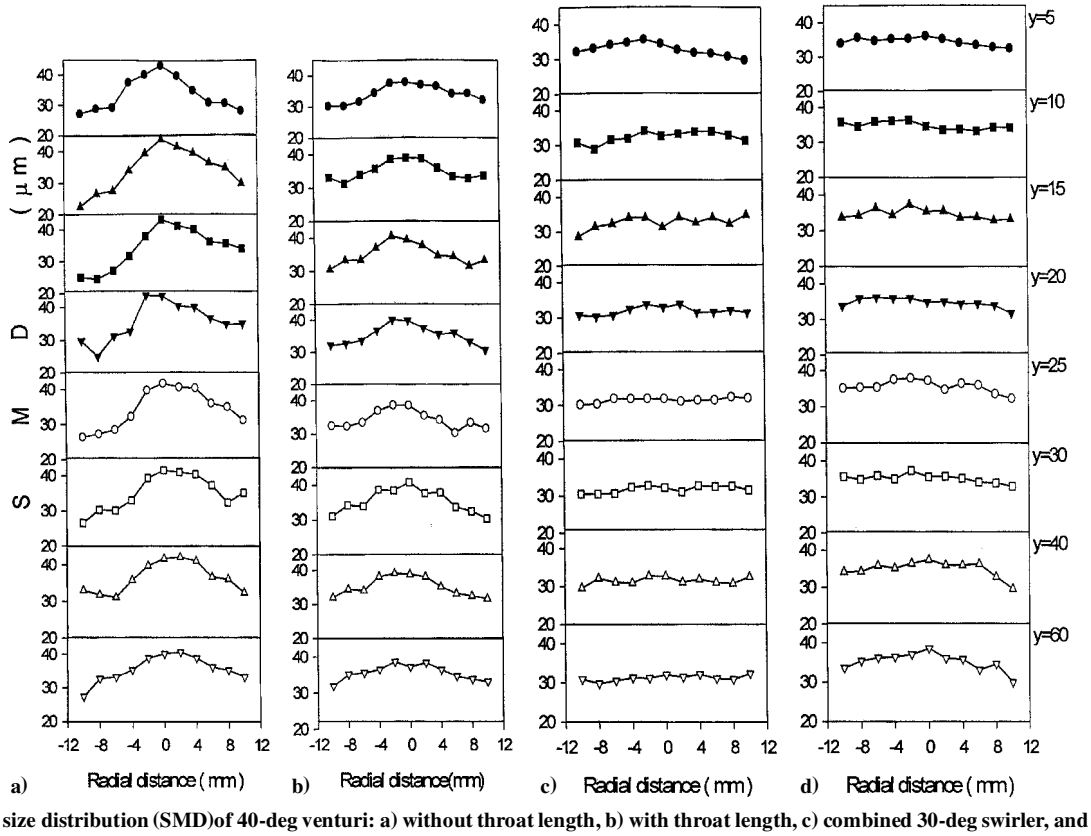


**Fig. 9 Droplet size distribution (SMD)of 40-deg venturi: a) without throat length, b) with throat length, c) combined 30-deg swirler, and d) 0.2-MPa ambient pressure on the throat length venturi.**

$2\alpha = 20, 40, 60$, and 80 deg; Figs. 10a–10d show the effects with a long-throat venturi and Figs. 10e–10h with a sharp-throat venturi. Figure 11 shows droplet size measurements at 5 mm from exit of the venturi tube in the radial direction. Similar to previously reported findings,[26,27] both the spray angles and SMD distribution were changed significantly with the venturi divergence angle and throat length. A longer venturi and, therefore, a longer residence time improve atomization and develop a more uniform spray distribution. However, too long a venturi tube may also bring about autoignition and wall-wetting problems.[27]

Figure 12 shows the effect of the swirler on a 40-deg venturi at 200-m/s air velocity and 0.1-MPa ambient pressure condition. When a swirler is added in front of the 40-deg venturi, the spray patterns widen significantly; however, too strong a swirler causes serious wall wetting and produces an asymmetric spray. The asymmetry is likely caused by the wake of the flow downstream of the swirl vane and

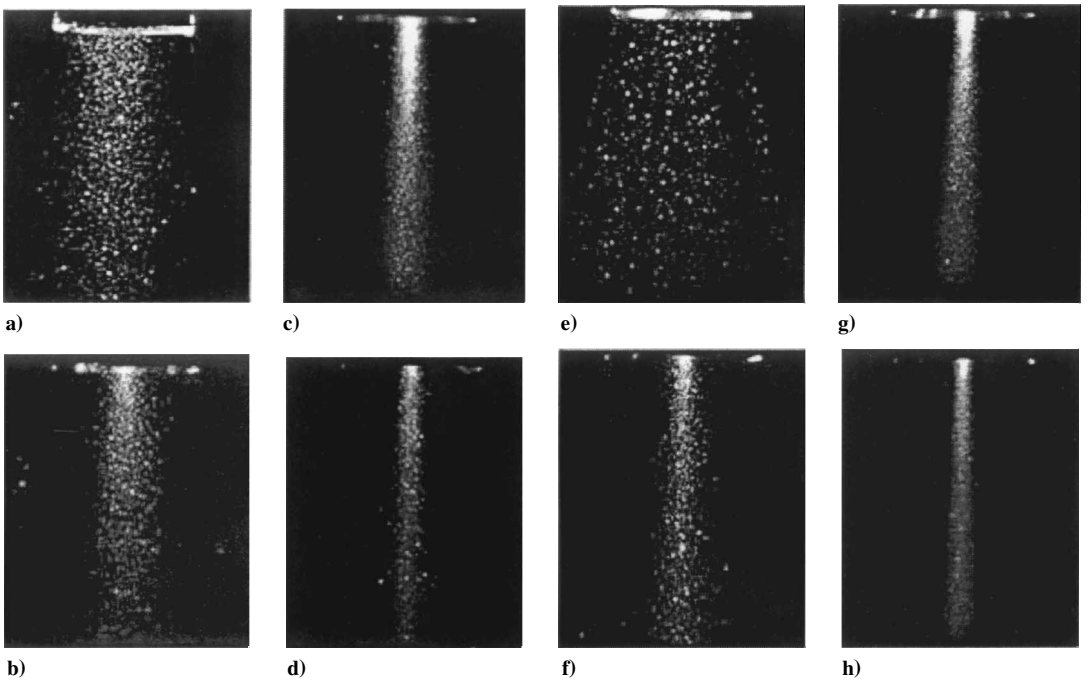


**Fig. 10 Effect of venturi geometry at air velocity 100 m/s and 0.1-MPa ambient pressure at divergence angle: a) 20-deg, b) 40-deg, c) 60-deg, and d) 80-deg venturi with throat length, and e) 20-deg, f) 40-deg, g) 60-deg, and h) 80-deg venturi without throat length.**

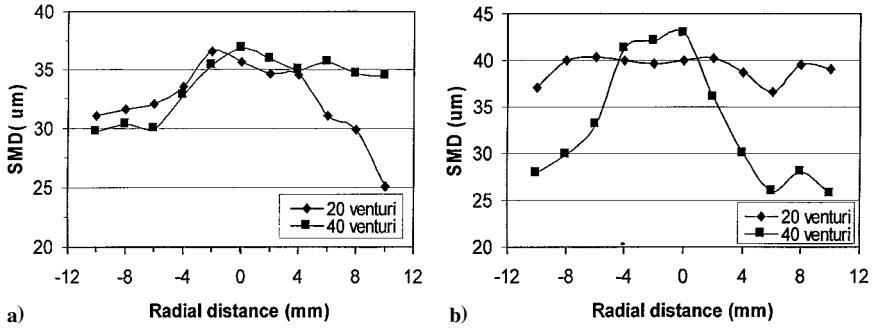


**Fig. 11 Droplet size distribution depending on venturi geometry: a) with throat length and b) without throat length.**

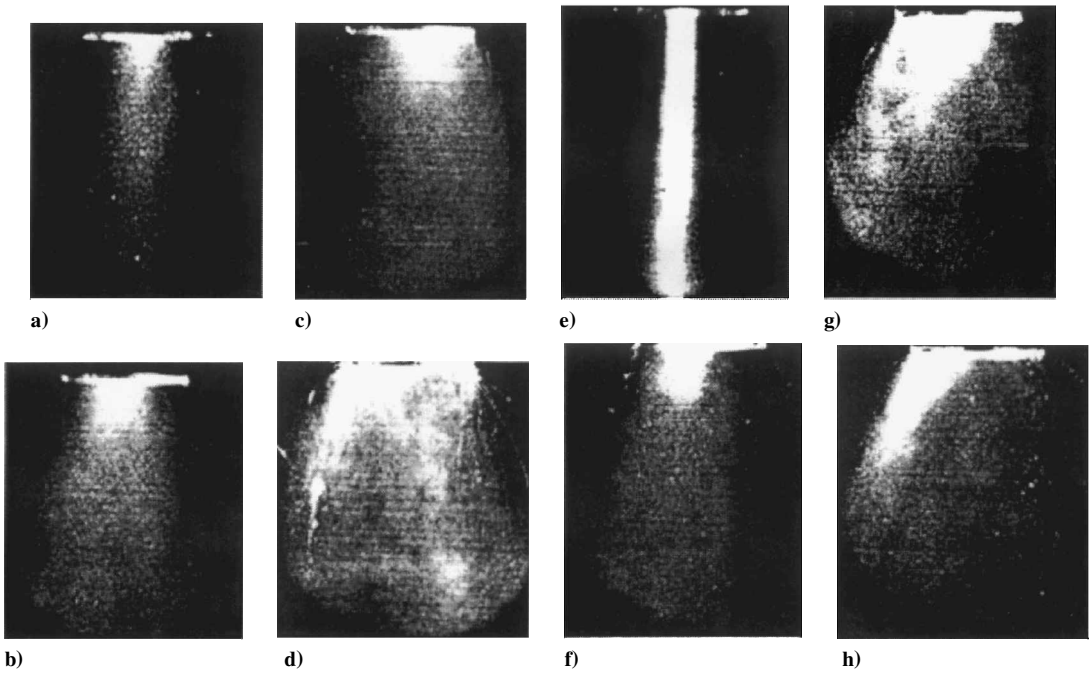


**Fig. 12 Effects of the swirler on the 40-deg venturi at air velocity 200 m/s and 0.1-MPa ambient pressure at vane angle: a) no swirler, b) 30-deg, c) 45-deg, and d) 60-deg with throat length, and e) no swirler, f) 30-deg, g) 45-deg, and h) 60-deg without throat length.**

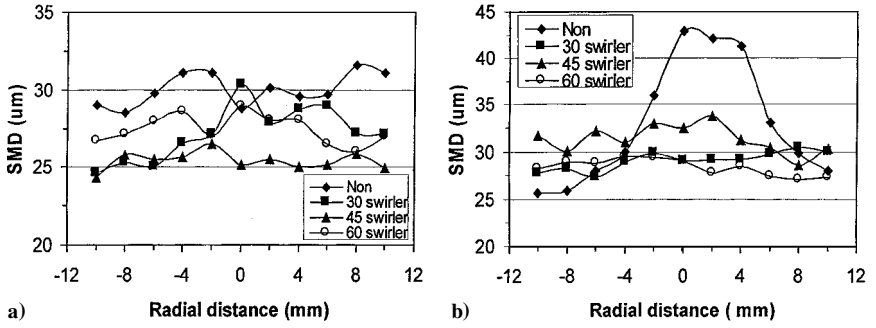


**Fig. 13 Droplet size distribution depending on different swirler: a) with throat length and b) without throat length.**

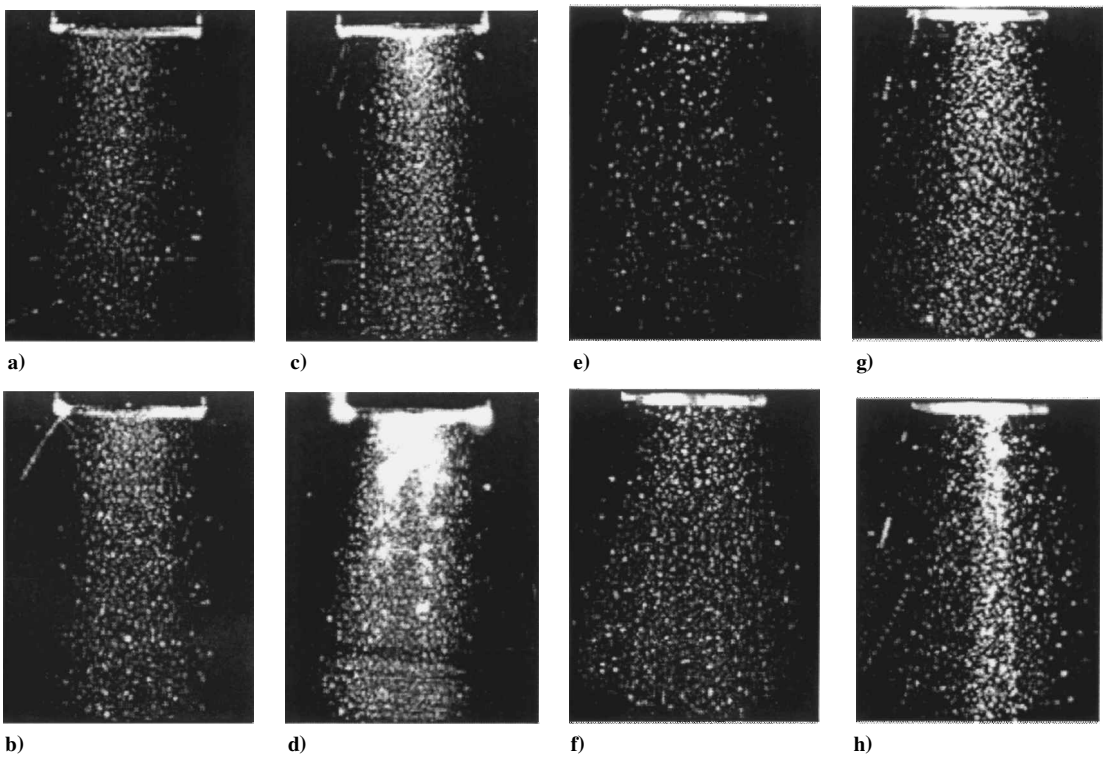


**Fig. 14 Effect of ambient chamber pressure without swirler on the 20-deg venturi at air velocity 100 m/s: a) 0.1 MPa, b) 0.2 MPa, c) 0.3 MPa, and d) 0.4 MPa with throat length, and e) 0.1 MPa, f) 0.2 MPa, g) 0.3 MPa, and h) 0.4 MPa without throat length.**

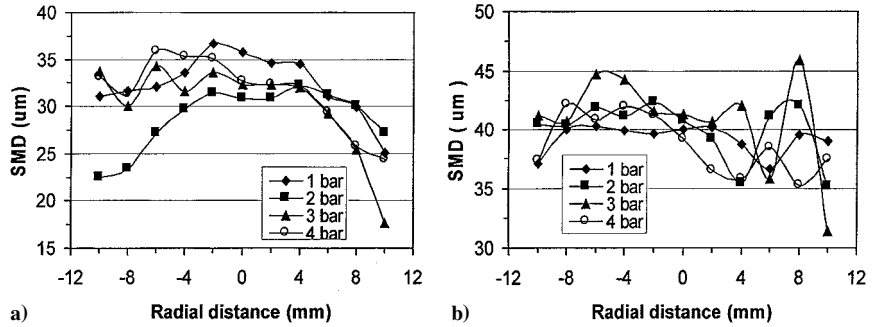


**Fig. 15 Droplet size distribution depending on ambient pressure without swirler effect: a) with throat length and b) without throat length.**

their precessions, which drive the spray stream to spiral outward and to impinge on the tube wall unevenly. In the case of a longer venturi with a 20-deg, divergent angle, wall impingement is also observed, although the spray becomes more uniform due to more even filming and secondary atomization. Results of the corresponding droplet size as shown in Fig. 13 are inconclusive; however, the long-throat 40-deg venturi with a 45-deg swirler seems to produce the smallest drop size evenly. Therefore, matching the venturi tube geometry with swirler angle is necessary to obtain optimal fuel atomization and distribution. However, a sufficiently long venturi tube with a mild swirler seems to be the best combination.

Earlier investigations on the effect of ambient pressure on spray atomization showed that the equivalent spray angle is inversely proportional to the ambient pressure. The phenomenon of decreasing spray angle is caused by increased aerodynamic drag on the liquid spray moving through the ambient gas.[28] Another study[21] developed

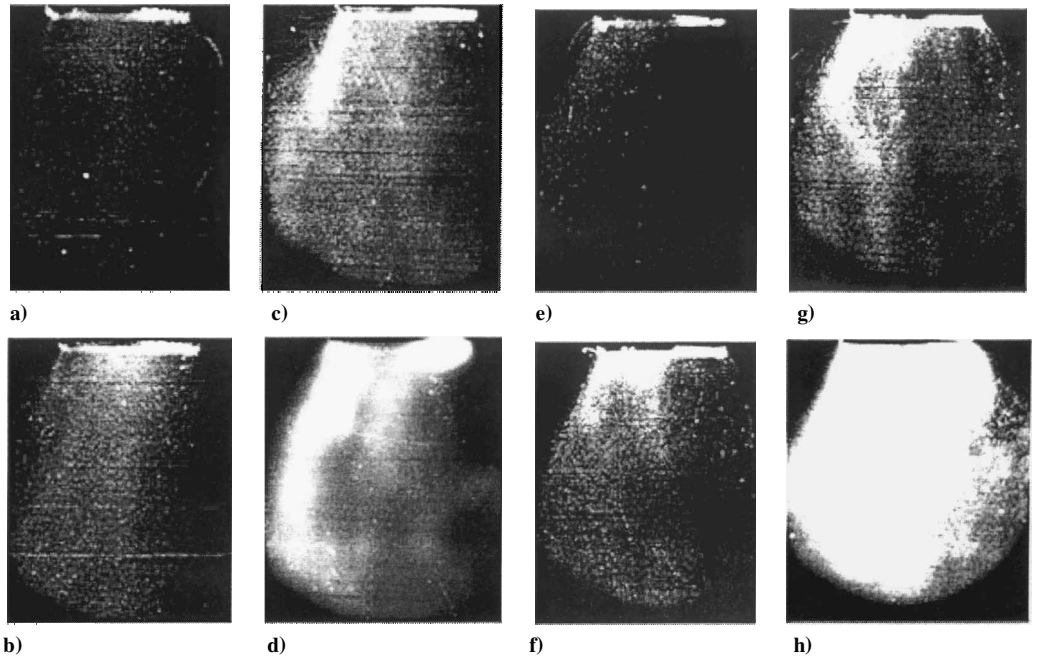


**Fig. 16 Effect of ambient chamber pressure with 45-deg swirler on the 40-deg venturi at air velocity 100 m/s: a) 0.1 MPa, b) 0.2 MPa, c) 0.3 MPa, and d) 0.4 MPa with throat length, and e) 0.1 MPa, f) 0.2 MPa, g) 0.3 MPa, and h) 0.4 MPa without throat length.**

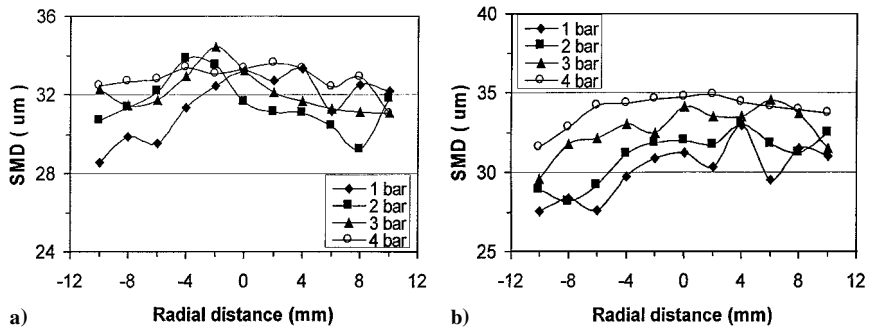


**Fig. 17 Droplet size distribution depending on ambient pressure with 45-deg swirler: a) with throat length and b) without throat length.**

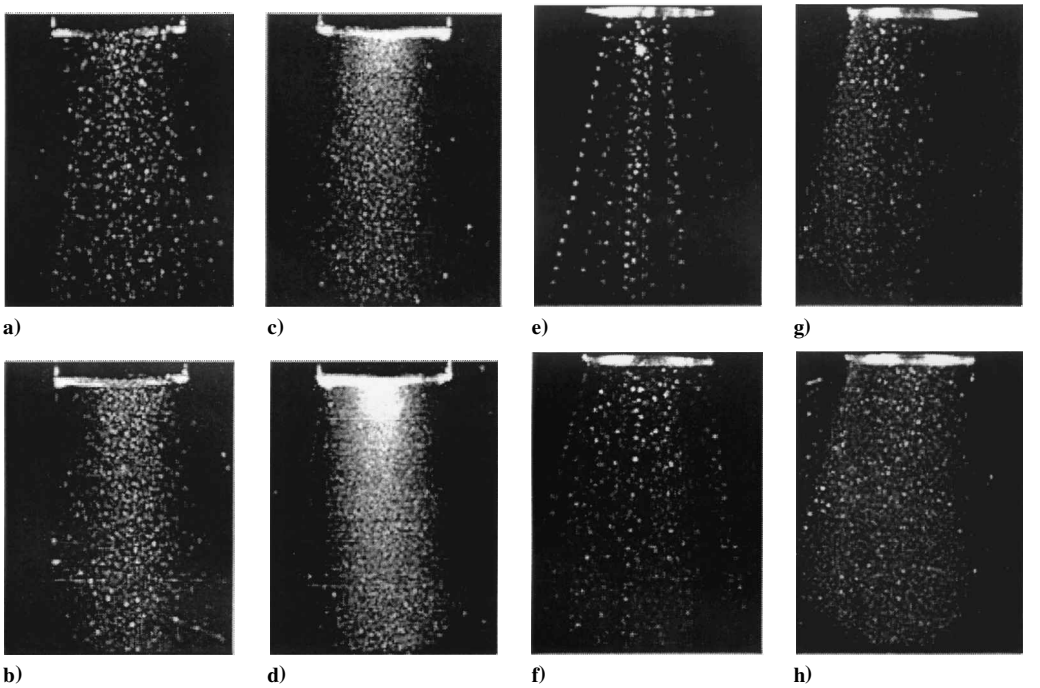


**Fig. 18 Effect of airflow rate on the 20-deg venturi at 0.1-MPa ambient pressure: a) 50 m/s, b) 100 m/s, c) 150 m/s, and d) 200 m/s with throat length, and e) 50 m/s, f) 100 m/s, g) 150 m/s, and h) 200 m/s without throat length.**

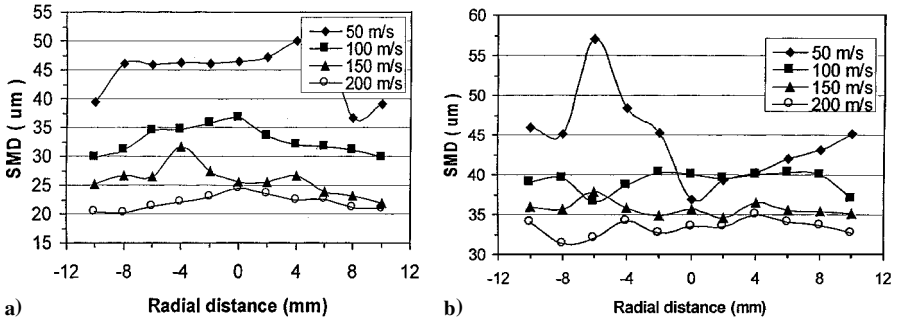


**Fig. 19 Droplet size distribution depending on different airflow rates (throat velocity): a) with throat length and b) without throat length.**

an empirical expression between the spray half-width and ambient gas pressure and concluded that the boundaries of the spray change from nearly straight to increasingly curvilinear in character as the chamber gas pressure increased. However, Zheng et al.[20] reported that increasing the ambient pressure of airblast atomizer sprays at constant fuel–air ratio caused the initial spray cone angle to widen, but the spray volume remained largely unaffected by the ambient pressure. Figure 14 shows the effect of ambient pressure on the spray from a 20-deg venturi injector, which has an averaged 100-m/s air velocity at the throat. Although the spray boundary does not change significantly, the spray density clearly increases to the center. The effect of ambient pressure on the droplet size as shown in Fig. 15 is also not clear. The situation may be complicated by competition between droplet breakup and the collision processes in the narrow and long venturi. The observed effects of the ambient pressure show good agreement with the Zheng et al. results.

In the case of combining the swirler on the venturi, some interesting results are shown in Figs. 16 and 17, for a 40-deg venturi with a $\theta = 45$ deg swirler, at 100-m/s throat air velocity condition. The increasing ambient pressure increases the spray density but does not seem to change the spray angle or make the asymmetric spray more symmetric for the pressure range tested. Figure 17 shows that the droplet size increased with ambient pressure in this wider spray.

Of all of the factors influencing the mean drop size, air velocity is undoubtedly the most important. Various investigations have shown from their empirical equations that the mean drop size for an airblast atomizer (including plain-jet airblast atomizer, simplex pressure swirl atomizer, prefilming airblast atomizer, etc.) decreases with an increasing air velocity. Similarly, the SMD of venturi nozzle spray decreases with airflow rate because of improved atomization at higher flow rate.[27,29]

Figures 18 and 19 show the effect of airflow rate for the 20-deg venturi at 0.1-MPa ambient pressure on the droplet size distribution and atomization. Qualitatively, the spray angle is less sensitive to variations in air velocity, but smaller spray droplet size and better atomization are observed in the original visualization images. As expected, the SMD at the lower velocity is largely due to poor atomization, as shown in Fig. 19. In the case with a finite throat length, the droplet size distribution at air velocity of 200 m/s decreases more than two times that at 50 m/s. This trend is similar in the zero-throat-length conditions, even though the spray is obviously asymmetric in low air speed conditions. Therefore, note that, at the high flow rate, better atomization produces a lot of small droplets, which will vaporize much faster than the large sized partners and, finally, enhance LPP combustor performance.

## Conclusion

The major conclusions from current study are summarized as follows.

1) The pressure drop across the venturi tube is dominated by throat velocity, divergent angle, and throat length; the effect of swirler on pressure drop is only important when the diffuser angle is small.

2) Matching the swirler with the venturi geometry is important to obtain optimal liquid atomization and droplet distribution.

3) Throat velocity is the most dominant parameter for drop size.

4) In general, a longer venturi tube results in wider spray angle and smaller drops than a shorter venturi tube.

5) Swirlers significantly widen the spray pattern and reduce the droplet size in the center of the spray.

6) Increasing ambient density increases droplet size and spray density significantly.

7) The venturi nozzle with finite throat length results in better atomization spray with a more uniform distribution than that without a throat length.

## Acknowlegment

The support of NASA John H. Glenn Research Center at Lewis Field, under Grant NAG3-1703 is appreciated.

## References

[1]Schorr, M. M., "$NO_x$ Emission Control for Gas Turbines: A 1992 Update on Regulations and Technology," *COGEN-TURBO*, IGTI-Vol. 7, American Society of Mechanical Engineers, Fairfield, NJ, 1992.

[2]Talpallikar, M. V., Smith C. E., Lai, M. C., and Holdeman, J., "CFD Analysis of Jet Mixing in Low $NO_x$ Flametube Combustors," *Journal of Engineering for Gas Turbines and Power*, Vol. 114, 1992, pp. 416–424; also NASA TM 104466, 1991.

[3]Zhu, G., Lai, M. C., and Lee, T., "Parametric Study of Penetration and Mixing of Radial Jets in Necked-Down Cylindrical Crossflow," *Journal of Propulsion and Power*, Vol. 11, No. 2, 1995, pp. 252–260.

[4]Cooper, L. P., "Effect of Degree of Fuel Vaporization upon Emissions for a Premixed Partially Vaporized Combustion System," NASA TP 1582, 1980.

[5]Correa, S.M., "Lean Premixed Combustion for Gas Turbine: Review and Required Research," *Fossil Fuel Combustion*, PD-Vol. 33, American Society of Mechanical Engineers, Fairfield, NJ, 1991.

[6]Lefebvre, A. H., "Pollution Control In Continuous Combustion Engines," *Fifthteenth (International) Symposium on Combustion*, Combustion Inst., Pittsburgh, PA, 1974, pp. 1169–1180.

[7]Davis, L. B., "Dry Low $NO_x$ Combustion System for GE Heavy-Duty Gas Turbines," *COGEN-TURBO*, IGTI-Vol.7, American Society of Mechanical Engineers, Fairfield, NJ, 1992.

[8]Davis, L. B., and Washam, P. E., "Development of a Dry Low $NO_x$ Combustor," American Society of Mechanical Engineers, ASME Paper 89-GT-255, 1989.

[9]Sattelmayer, T., Felchlin, M. P., Haumann, J., Hellat, J. M., and Styner, D., "Second-Generation Low-Emission Combustors for ABB Gas Turbines: Burner Development and Tests at Atmospheric Pressure," *Journal of Engineering for Gas Turbines and Power*, Vol. 114, 1992, p. 118.

[10]Tacina, R. R., "Low $NO_x$ Potential of Gas Turbine Engines," AIAA Paper 90-0550, 1990.

[11]Viereck, D., Wettstwin, H. E., Aigner, M., and Kiesow, H. J., "The Cleanest Gas Turbine for Combined Cycle and Cogeneration Application," *COGEN-TURBO*, IGTI-Vol. 7, American Society of Mechanical Engineers, Fairfield, NJ, 1992.

[12]Yule, A. J., and Damou, M., "Axisymmetrical Turbulent Jet Flows In a Duct of Varying Area," *Experimental Thermal and Fluid Science,* Vol. 5, No. 4, 1992, pp. 580–591.

[13]Lyons, V. J., "Fuel/Air Nonuniformity-Effect of Nitric Oxide Emissions," *AIAA Journal*, Vol. 20, No. 5, 1982, pp. 660–665.

[14]Tacina, R. R., "Experimental Evaluation Fuel Preparation Systems for an Automotive Gas Turbine," NASA TM-7885, 1977.

[15]Tacina, R. R., "Performance of a Multiple Venturi Fuel Air Preparation System," NASA CP-2078, 1979.

[16]Johnson, S. M., "Venturi Nozzle Effects on Fuel Drop Size and Nitrogen

Oxide Emissions," NASA TP 2028, 1982.

[17]Ercegovic, D. B., "Effect of Swirler-Mounted Mixing Venturi on Emissions of Flame-Tube Combustor Using Jet A Fuel," NASA TP 1393, 1979.

[18]Rizk, N. K., "Spray Characteristic of Plain Jet Airblast Atomizers," *Journal of Engineering for Gas Turbines and Power*, Vol. 106, 1984, pp. 634–638.

[19]Lefebvre, A. H., *Gas Turbine Combustion*, Hemisphere, New York, 1983.

[20]Zheng, Q. P., Jasuja, A. K., and Lefebvre, A. H., "Structure of Airblast Sprays Under High Ambient Pressure Conditions," *Journals of Engineering for Gas Turbines and Power*, Vol. 119, 1997, pp. 512–518.

[21]Parsons, J. A., and Jasuja, A. K., "Effect of Air Pressure Upon Angle/Width Characteristics of Simplex Pressure Swirl Atomizers," *International Journal of Turbo and Jet Engines 3*, 1986, pp. 207–216.

[22]Bachalo, W. D., Rudoff, R. C., and Brena de la Rosa, A., "Mass Flux Measurements of a High Number Density Spray System Using the Phase Doppler Droplet Analyzer," AIAA Paper 88-0236, 1988.

[23]O'Rouke, P. J., and Amsden, A., "The TAB Method for Numerical Calculation of Spray Droplet Breakup," Society of Automotive Engineers, Rept. SAE 872089, 1987.

[24]Przekwa, A., Chuech, S., and Singhal, A., "Numerical Modeling for Primary Atomization of Liquid Jets," AIAA Paper 89-0163, 1989.

[25]Reitz, R. D., "Modeling Atomization Processes in High-Pressure Vaporizing Sprays," *Atomization and Spray Technology*, Vol. 3, 1987, pp. 309–337.

[26]Sun, H., Chue, T. H., Lai, M. C., and Tacina, R., "Atomization Characteristics of Capillary Fuel Injection Inside a Venturi Nozzle," *Atomization and Sprays*, Vol. 7, 1997, pp. 245–265.

[27]Sun, H., Chue, T. H., Lai, M. C., and Tacina, R. R., "Atomization and Vaporization Characteristics of Airblast Fuel Injection Inside a Venturi Tube," AIAA Paper 93-1766, 1993.

[28]Lefebvre, A. H., *Atomization and Sprays*, Hemisphere, New York, 1989.

[29]Hardalupas, Y., and Whitelaw, J. H., "Characteristics of Sprays Produced by Coaxial Airblast Atomizers," *AIAA Journal*, Vol. 10, No. 4, 1993, pp. 453–459.